While the chemical reversibility of the oxidations of (TPP)ZnL in $EtCl_2$ seen here is interesting, it is at variance with previously reported work in acetonitrile. It is surprising that no measurable quantity of the (β-py) derivative is formed and suggests that the solvent system plays an important role in the intermediate stablization of two possible oxidative pathways. Since the isolation of the (β-py) derivative was easily repeated and the $[(TPP)ZnL]^+$ titration showed mixed species spectra, this solvent effect must indeed be operative. It should be noted, however, that even with the 500-ms time scale of our spectral acquisitions we cannot determine the exact nature of the intermediates in these pathways. Spectral changes were instantaneous with ligand addition.

Acknowledgment. The support of this research from the National Science Foundation (Grant CHE-7921536) and the Robert A. Welch Foundation (Grant E-680) is gratefully acknowledged. The authors also wish to thank Mr. Randy Wilkins for construction of the bulk coulometry cell.

Registry No. (TPP)Zn, 14074-80-7; $[(TPP(\beta\text{-py}))Zn]^+(ClO_4^-)$, 60165-30-2; py, 110-86-1; 3,4-lutidine, 583-58-4; 3,4-dichloropyridine, 55934-00-4; 4-(dimethylamino)pyridine, 1122-58-3; 3-bromopyridine, 626-55-1; MeOH, 67-56-1.

Contribution from the Laboratoire de Cristallochimie et de Chimie Structurale, Université Louis Pasteur, Institut Le Bel, 67070 Strasbourg, France, and the Laboratoire CNRS-SNPE, 94320, Thiais, France

Molecular Structure of Phosphaferrocene and Charge Density Distribution at Low Temperature

R. WIEST, B. REES,* A. MITSCHLER, and F. MATHEY

Received December 23, 1980

X-ray diffraction measurements have been performed at 74 K on the sandwich complex dimethylphosphaferrocene. The molecular geometry is discussed and compared to room-temperature results. A qualitative study of the charge density distribution (X–X method) shows an analogy with ferrocene in the metal region. A strong peak in the phosphorus region is indicative of a localized lone pair. This is in apparent contradiction with the electrophilic character of phosphorus, deduced from chemical and spectral properties.

A chemical and spectroscopic (NMR and mass spectra) study of phosphaferrocene has demonstrated the aromaticity of the phospholyl group in this complex, in sharp contrast to uncomplexed phospholes C_4H_4PR.[1] Thus, whereas phosphole acetylation takes place at the P atom, phosphaferrocene is exclusively acetylated on the C atoms of the phospholyl nucleus. The question was asked whether the electrophilic character of phosphorus in the complex implied a delocalization of the P lone pair.

In an attempt to answer this question, we performed low-temperature X-ray diffraction measurements in order to determine experimentally the charge density distribution in dimethylphosphaferrocene (X–X method). The crystal structure of the same compound had already been determined at room temperature.[2]

Experimental Section

A crystal of the title compound has been grown by sublimation under vacuum at 40 °C and ground into a sphere. A few general and crystallographic data are given in Table I. There is no phase change between room temperature and 74 K. The low-temperature cell dimensions were determined by accurate centering of 12 reflections and their Friedel equivalents at $+2\theta$ and -2θ (Mo $K\alpha_1$, $65° < 2\theta < 70°$).

Details of the experimental conditions are given in Table II. The measurements were performed on a Picker diffractometer equipped with a beryllium cryostat. A stable temperature of 74 K was maintained by circulation of liquid nitrogen under depression.

Three standard reflections were measured after every 60 regular measurements. The variation of their intensity as a function of time was used to determine an overall time-dependent scale factor. A locally written Fortran program (STANDARD) was used for this purpose. Values of the scale factor (and its esd) are obtained by averaging over groups of ten consecutive standard reflection intensities. Linear interpolation is then used to determine the scale factor of any given reflection and to modify accordingly the esd of its intensity. This procedure also enables to estimate the variance σ^2 of individual intensities before scaling from the observed dispersion within each group

Table I. General and Crystallographic Characteristics for (η^5-Cyclopentadienyl)[η^5-(3,4-dimethyl-1-phosphacyclopentadienyl)]iron

formula $(\eta^5\text{-}C_5H_5)[\eta^5\text{-}PC_4H_2(CH_3)_2]Fe$ or $C_{11}H_{13}PFe$; $M_r = 232.04$

monoclinic, space group $P2_1/n$;[a] $Z = 4$

cell dimensions at 293 K:[2] $a = 12.292$ (4) Å, $b = 10.824$ (3) Å, $c = 7.831$ (2) Å, $\beta = 91.60$ (4)°, $V = 1041.5$ Å^3, $\rho_{calcd} = 1.48$

cell dimensions at 74 K: $a = 12.092$ (1) Å, $b = 10.667$ (1) Å, $c = 7.767$ (1) Å, $\beta = 91.73$ (1)°, $V = 1001.4$ Å^3, $\rho_{calcd} = 1.54$

[a] In ref 2, the space group was mistakenly reported as $P2_1/c$.

Table II. Diffraction Measurements and Data Processing

wavelength = 0.709 30 Å (Mo $K\alpha_1$)
temp = 74.0 ± 0.5 K
sample size: diameter = 0.24 ± 0.01 mm
absorptn: $\mu = 16.10$ cm^{-1}; transmission factor between 0.751 and 0.758
monochromator: graphite; $2\theta_{min} = 11.66°$
continuous $\omega/2\theta$ scan; speed in $2\theta = 2°$/min
scan interval in 2θ: $2.3° + \alpha_1\alpha_2$ separation
bkgd measurement: during 20 s at each end of the scan interval
no. of measured reflctns: 14853 (2 crystallographically equivalent sets); 3635 independent reflections with $(\sin\theta)/\lambda < 0.76$ Å^{-1}; 3976 independent reflections with $(\sin\theta)/\lambda > 0.76$ Å^{-1}
agreement between equivalent reflections: $R = \Sigma(|I - \langle I\rangle|)/\Sigma\langle I\rangle = 0.046$ (0.023 for $(\sin\theta)/\lambda < 0.76$ Å^{-1})

* To whom correspondence should be addressed at the Université Louis Pasteur.

(1) Mathey, F. *J. Organomet. Chem.* **1977**, *139*, 77-87.
(2) Mathey, F.; Mitschler, A.; Weiss, R. *J. Am. Chem. Soc.* **1977**, *99*, 3538.

0020-1669/81/1320-2966$01.25/0

Table III. Relative Coordinates ($\times 10^5$) and Thermal Motion Parameters ($\times 10^4$ Å^2)[a]

	x	y	z	U_{11}	U_{22}	U_{33}	U_{12}	U_{13}	U_{23}
Fe	24398 (4)	11696 (3)	2199 (4)	125 (1)	87.7 (6)	74.4 (5)	−6 (1)	1.1 (7)	−4.3 (8)
P	11018 (7)	22174 (7)	16528 (10)	117 (3)	170 (2)	155 (2)	11 (2)	26 (2)	3 (2)
C(1)	21328 (24)	13562 (19)	28169 (28)	151 (9)	134 (6)	103 (5)	−12 (5)	11 (6)	1 (4)
C(2)	32342 (23)	17309 (20)	24689 (26)	147 (8)	122 (5)	100 (5)	6 (5)	−14 (6)	−9 (4)
C(3)	32525 (23)	32525 (23)	27134 (19)	156 (8)	95 (5)	129 (5)	−5 (5)	3 (6)	−9 (4)
C(4)	21664 (24)	30507 (19)	6252 (32)	145 (8)	110 (5)	144 (6)	1 (5)	3 (6)	9 (5)
C(5)	42365 (25)	11745 (32)	33701 (30)	183 (9)	200 (7)	140 (6)	30 (8)	−43 (7)	3 (7)
C(6)	42831 (28)	33178 (26)	5789 (44)	140 (9)	174 (8)	231 (9)	−33 (6)	38 (8)	12 (6)
C(7)	22648 (38)	−7016 (22)	−3756 (31)	336 (15)	115 (6)	130 (7)	−36 (7)	16 (8)	−4 (5)
C(8)	33657 (35)	−3021 (27)	−5995 (37)	253 (13)	166 (7)	161 (7)	70 (8)	2 (8)	−30 (6)
C(9)	33550 (32)	6859 (26)	−18447 (34)	216 (12)	182 (8)	135 (6)	−14 (7)	38 (8)	−25 (5)
C(10)	22307 (33)	9048 (27)	−2390 (30)	256 (14)	178 (7)	104 (5)	−8 (7)	−9 (7)	−1 (5)
C(11)	15644 (34)	341 (30)	−14801 (35)	251 (13)	207 (8)	143 (7)	−79 (8)	−45 (8)	−17 (6)

	x	y	z	U, Å^2		x	y	z	U, Å^2
H(1)	19742 (119)	7132 (136)	35769 (185)	176 (37)	H(63)	44870 (137)	39690 (157)	13288 (216)	323 (46)
H(4)	20463 (123)	36466 (130)	−2397 (180)	156 (36)	H(7)	19905 (149)	−12688 (156)	3219 (220)	360 (48)
H(51)	48843 (134)	12368 (142)	26736 (208)	262 (41)	H(8)	40159 (124)	−6576 (141)	27 (193)	223 (40)
H(52)	41174 (143)	3553 (176)	36098 (232)	426 (53)	H(9)	39889 (136)	11494 (149)	−22505 (215)	328 (45)
H(53)	43959 (134)	16112 (156)	43794 (220)	288 (44)	H(10)	19565 (124)	15560 (144)	−32052 (192)	207 (39)
H(61)	41714 (126)	36311 (142)	−5342 (204)	213 (39)	H(11)	8079 (131)	475 (150)	−15722 (199)	269 (43)
H(62)	49216 (131)	27171 (152)	5343 (201)	259 (43)					

[a] The parameters of the nonhydrogen atoms are from a high-order least-squares refinement ($(\sin\theta)/\lambda > 0.76$ Å^{-1}). The temperature factor is $\exp(-2\pi^2\Sigma_i\Sigma_j U_{ij}h_i a_i^* h_j a_j^*)$. Esd's are for the rightmost digits.

of ten intensities. This may be compared to the value due to the counting statistics alone, σ_c^2. It was found that the usual expression $\sigma^2 = \sigma_c^2 + p^2I^2$ could be used only if p was assumed to be a function of sin χ (probably because the weight of the nitrogen transfer line causes some mechanic instability for χ values close to ±90°).

After the usual corrections, the intensity of crystallographically equivalent reflections was averaged. A conventional least-squares refinement of the atomic parameters and the crystallographic scale factor k was performed in which all reflections with $I/\sigma > 3$ were used. The quantity minimized was $\sum(|kF_c|^2 - F_o^2)^2/\sigma^2$. The atomic scattering factors and the dispersion constants were taken from ref 3. The extinction was found negligible. Agreement indices had the following values: $R(F) = 0.038$, $R_w(F) = 0.031$, and goodness of fit (GOF) = 1.44.

The observed intensities were then split into two sets. Low-order reflections ($(\sin\theta)/\lambda < 0.76$ Å^{-1}) were used to calculate the electron density, as will be discussed below. High-order data ($(\sin\theta)/\lambda > 0.76$ Å^{-1}) were used to determine positional and thermal parameters for the nonhydrogen atoms, hopefully unbiased by bonding effects. All high-order reflections, even those of negative observed intensity, were included in this calculation. The scale factor was kept at the value given by the conventional refinement to avoid large correlations with the thermal parameters. Agreement indices were $R(F) = 0.155$, $R_w(F) = 0.072$, and GOF = 0.96. The small value of the GOF is an indication of the validity of the spherical-atom model for the high-order refinement and of the general correctness of the esd's of the data. The refined atomic parameters are reported in Table III.

Molecular Geometry

Details on the molecular geometry at both low temperature (74 K, this work) and room temperature[2] are given in Tables IV–VI. The bond lengths were corrected for the apparent shortening due to thermal librational motion, in the rigid body approximation, considering the separate fragments FeCp and FePh (hereafter the cyclopentadienyl ring is represented by Cp and the dimethylphospholyl ring by Ph). The thermal motion of the molecule may be decomposed into roughly isotropic translational and librational vibrations, *plus* an extra libration of the Cp ring around its axis. The root-mean-square amplitudes of the former vibrations are about 0.1 and 0.2 Å at low and room temperature, respectively, for the translations and 2.5 and 5° for the librations so that the square amplitudes are approximately proportional to the absolute temperature. The amplitude of the extra angular motion of the Cp ring is 3.6° at 74 K and 10.3° at room temperature. Analogous vibrational behavior has been observed in the low-temperature phase of ferrocene[4] where the extra amplitude, extrapolated to 74 K, is 3.0°, thus indicating that the torsional force constant is approximately the same in both compounds. This angular motion causes a larger apparent shortening of the bond lengths in the FeCp group than in FePh, especially at room temperature. No extra motion of the Ph ring around the normal to its plane is noticed, probably because of the presence of the methyl groups.

The corrected bond lengths and bond angles, as observed at the two temperatures, are in good agreement. The two fragments FeCp and FePh are essentially symmetric through the planes FeΩ(Cp)C(11) and FeΩ(Ph)P, respectively, where Ω(Cp) and Ω(Ph) are the centers of the rings. The two planes, however, make a small angle which measures the deviation from the exactly eclipsed conformation and may be calculated as the mean value of the five dihedral angles A(Cp)Ω(Cp)Ω(Ph)A(Ph) (where the A's are nearly eclipsed atoms). The most significant change between the room-temperature and the low-temperature conformation is the increase of this angle from 0.85 (10) to 1.70 (5)° (Table V). The larger distortion at low temperature is consistent with the stronger intermolecular interactions, as seen from the contraction of the cell dimensions (Table I); since the intramolecular dimensions remain practically unchanged, an average shortening of about 0.1 Å of the intermolecular distances may be inferred.

The Ph ring is not planar, the P atom being displaced by 0.05 Å out of the plane of the C atoms away from the metal (Table VI). The methyl carbon atoms are displaced in the same direction by about 0.02 Å.

The C atoms of the Cp ring form a regular and planar pentagon within the limits of experimental errors. The mean C–C bond length (1.431 Å) is identical with the value observed in crystallized ferrocene[4] and with an earlier electron diffraction result for the same compound in the vapor phase,[5] slightly less than a redetermined value (1.440 ± 0.002 Å[6]). The plane is not exactly parallel to the carbon plane of the

(3) "International Tables for X-ray Crystallography"; Kynoch Press: Birmingham, England, 1974; Vol. IV.

(4) Seiler, P.; Dunitz, J. *Acta Crystallogr., Sect. B* **1979**, *B35*, 2020–2032.
(5) Bohn, R. K.; Haaland, A. *J. Organomet. Chem.* **1966**, *5*, 470–476.
(6) Haaland, A.; Nilson, J. E. *Acta Chem. Scand.* **1968**, 2653–2670.

Table IV. Interatomic Distances (Å) at Room Temperature[a] and at 74 K

	uncor		cor for thermal motion	
	room temp	74 K	room temp	74 K
	Phospholyl			
Fe-P	2.276 (1)	2.284 (1)	2.291	2.287
Fe-C(1)	2.064 (4)	2.072 (2)	2.077	2.075
Fe-C(2)	2.046 (4)	2.057 (2)	2.060	2.060
Fe-C(3)	2.040 (4)	2.054 (2)	2.055	2.057
Fe-C(4)	2.051 (4)	2.060 (2)	2.065	2.063
P-C(1)	1.758 (5)	1.774 (3)	1.770	1.777
P-C(4)	1.768 (5)	1.774 (3)	1.781	1.777
C(1)-C(2)	1.408 (7)	1.424 (4)	1.419	1.427
C(3)-C(4)	1.403 (7)	1.422 (4)	1.413	1.424
C(2)-C(3)	1.414 (6)	1.436 (3)	1.424	1.438
C(2)-C(5)	1.503 (8)	1.503 (3)	1.514	1.506
C(3)-C(6)	1.516 (8)	1.498 (4)	1.528	1.500
C(1)-H(1)	0.92 (7)	0.93 (1)[a]		
C(4)-H(4)	0.90 (7)	0.93 (1)		
C(5)-H(51)	0.90 (7)	0.97 (2)		
C(5)-H(52)	0.80 (7)	0.91 (2)		
C(5)-H(53)	1.02 (7)	0.93 (2)		
C(6)-H(61)	0.82 (8)	0.93 (2)		
C(6)-H(62)	0.98 (7)	1.00 (2)		
C(6)-H(63)	0.95 (7)	0.93 (2)		
	Cyclopentadienyl			
Fe-C(7)	2.046 (6)	2.058 (2)	2.072	2.065
Fe-C(8)	2.036 (7)	2.041 (3)	2.060	2.047
Fe-C(9)	2.077 (6)	2.042 (3)	2.045	2.046
Fe-C(10)	2.039 (5)	2.055 (2)	2.055	2.059
Fe-C(11)	2.045 (4)	2.061 (2)	2.068	2.067
C(11)-C(7)	1.399 (10)	1.423 (5)	1.427	1.428
C(11)-C(10)	1.393 (10)	1.430 (5)	1.421	1.435
C(7)-C(8)	1.378 (12)	1.414 (6)	1.408	1.419
C(9)-C(10)	1.412 (10)	1.431 (6)	1.442	1.437
C(8)-C(9)	1.411 (9)	1.430 (5)	1.438	1.435
C(7)-H(7)	0.70 (7)	0.88 (2)		
C(8)-H(8)	0.89 (7)	0.98 (2)		
C(9)-H(9)	1.02 (7)	0.97 (2)		
C(10)-H(10)	1.06 (7)	0.99 (2)		
C(11)-H(11)	0.70 (7)	0.92 (2)		

[a] The esd's are for random errors only. The systematic shortening due to the asphericity of the electron distribution around the H nuclei is not considered.

Table V

		room temp	74 K
	Bond Angles (Deg)		
phospholyl	C(1)-P-C(4)	88.4 (3)	88.9 (2)
	P-C(1)-C(2)	114.1 (3)	113.9 (2)
	P-C(4)-C(3)	113.9 (3)	114.0 (2)
	C(1)-C(2)-C(3)	111.7 (4)	111.6 (2)
	C(2)-C(3)-C(4)	111.9 (4)	111.6 (2)
	C(5)-C(2)-C(1)	123.5 (5)	123.1 (2)
	C(5)-C(2)-C(3)	124.8 (5)	125.3 (2)
	C(6)-C(3)-C(2)	125.1 (5)	124.5 (2)
	C(6)-C(3)-C(4)	123.1 (5)	123.9 (5)
cyclopentadienyl	C(7)-C(11)-C(10)	108.8 (7)	108.8 (3)
	C(11)-C(7)-C(8)	108.5 (7)	107.8 (3)
	C(11)-C(10)-C(9)	106.9 (6)	107.0 (3)
	C(7)-C(8)-C(9)	107.8 (7)	108.4 (3)
	C(8)-C(9)-C(10)	108.1 (6)	108.0 (3)
	Dihedral Angles (Deg)[a]		
	Cp, C(1)C(2)C(3)C(4)	3.2 (2)	3.5 (1)
	Cp, C(1)PC(4)	4.9 (2)	5.6 (1)

[a] Deviation from eclipsed position: room temp, 0.85 (10)°; 74 K, 1.70 (5)°.

Ph ring but makes an angle of 3.5° about a direction which is nearly perpendicular to the molecule mirror plane. The H atoms are generally displaced out of the plane toward the metal. Such an umbrella conformation may improve the d(metal)–pπ(ligand) overlap, as discussed by Elian et al.[7]

Table VI. Distances (Å) from Molecular Planes

	room temp	74 K
	Plane C(1)C(2)C(3)C(4)	
C(1)–C(4)	0.001[a]	0.001[a]
P	0.041 (3)	0.048 (1)
C(5)	0.016 (7)	0.028 (3)
C(6)	0.016 (7)	0.014 (3)
H(1)	−0.07 (7)	−0.03 (1)
H(2)	0.01 (7)	−0.05 (1)
Fe	−1.625 (3)	−1.625 (1)
Fe (cor)	−1.635	−1.628
	Plane C(7)C(8)C(9)C(10)C(11)	
C(7)–C(11)	0.002[a]	0.003[a]
H(7)	0.08 (7)	0.03 (2)
H(8)	0.05 (7)	0.00 (2)
H(9)	0.04 (7)	0.01 (2)
H(10)	0.06 (7)	0.04 (2)
H(11)	0.12 (8)	0.06 (2)
Fe	1.655 (3)	1.654 (2)
Fe (cor)	1.664	1.658

[a] Root mean square.

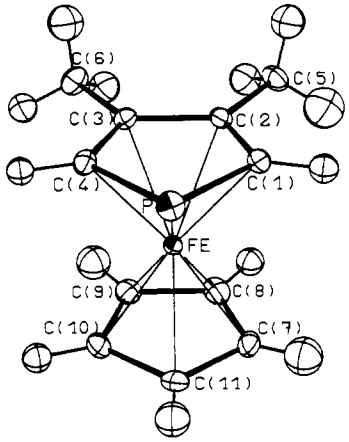

Figure 1. Molecular structure at 74 K. The thermal ellipsoids correspond to 50% probability.

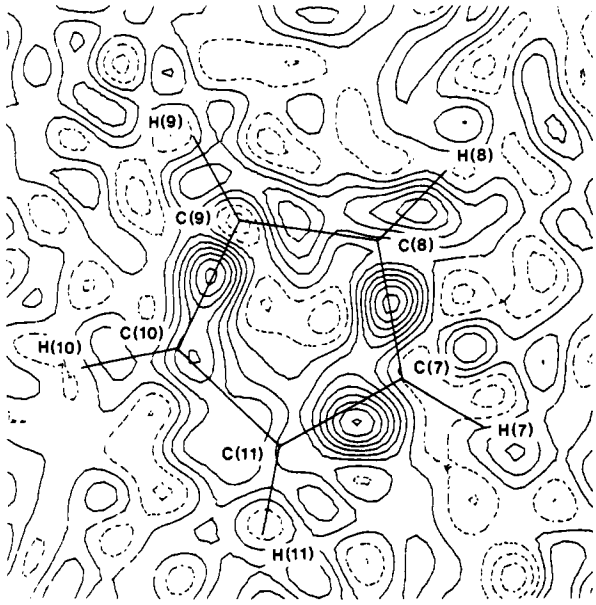

Figure 2. Deformation density in the plane of the cyclopentadienyl ring. The spacing of contour levels is 0.1 e Å^{-3}; negative contours are dashed.

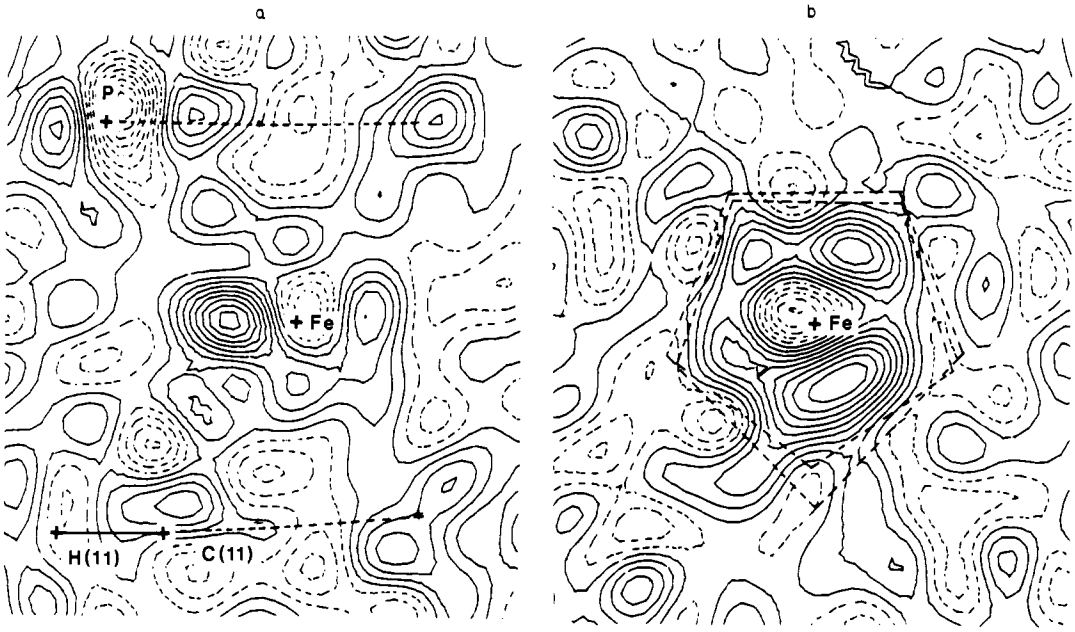

Figure 3. Deformation density in two planes containing the iron nucleus: (a) plane passing through P and C(11); (b) plane parallel to the Cp ring. Contours are as in Figure 2.

These authors have shown that the angular displacement should be negative (away from the metal) for the smallest rings and increase with the number of carbon atoms of the ring. With the use of the same kind of argument, a tilting of the normal to the Cp plane away from the molecular axis Fe–Ω-(Ph) improves the overlap of C(8) and C(9) with the metal orbitals and worsens that of C(11) so that, in order to compensate, the displacement of H(11) should be larger than that of H(8) and H(9). This is indeed observed, although the large uncertainty of the H positions makes it hardly significant.

Charge Density

The deformation density (total density *minus* free spherical atoms) was calculated with all reflections such that $(\sin\theta)/\lambda < 0.76$ Å^{-1}. The same set of reflections was used to determine the scale factor by scaling the observed structure factors on the calculated ones. The atomic parameters used in those calculations were those of Table III (high-order refinement for the nonhydrogen atoms).

The density maps obtained in this way (commonly called X–X maps) displayed an unusually high level of background noise. The esd of the observed density in general position was 0.12 e Å^{-3}. A Fortran program was written for the computation of the Fourier transform of this residual density, excluding the atomic regions, in an attempt to trace the observed high background to a wrong value of some particular structure factors. But the residues so obtained appeared more or less randomly distributed among all reflections. It seemed thus likely that the errors were essentially random. The reason could be the relatively poor quality of the crystals available. We also calculated the deformation density excluding the weakest reflections and/or those with large esd's. This reduced the background level but also changed the height of the peaks, thus indicating that such a procedure introduces systematic effects and should therefore be avoided.

The essential features of the deformation density are, however, clearly visible. Sections by some relevant planes are shown in Figures 2–4. The asphericity of the charge density around the metal is seen in the two perpendicular planar sections of Figure 3 and in the spherical section of Figure 5:

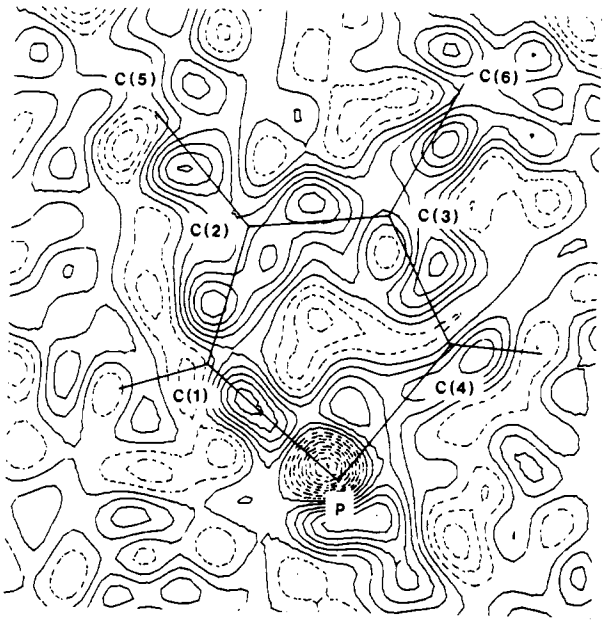

Figure 4. Deformation density in the phospholyl ring (plane of the C atoms). Contours are as in Figure 2.

this is a stereographic projection of the deformation density on a sphere centered on the iron nucleus. Figure 3 shows that most features in the metal region peak at a distance of about 0.65 Å from the nucleus; this value was therefore chosen as the radius of the sphere. The maximum of the radial part of 3d-electron distributions occurs at shorter distance but is displaced to about this value due to thermal motion and limited resolution.[8] The electron density around Fe is essentially characterized by an accumulation in the equatorial plane (parallel to the cyclopentadienyl and the phospholyl ring) and in the direction perpendicular to this plane (toward the center of the two rings). The deformation density is generally negative in the direction of the C and P atoms. Such a distribution is indicative of a population of the d_{z^2}, d_{xy}, and $d_{x^2-y^2}$ orbitals larger than that of the d_{xz} and d_{yz} orbitals. In this respect

(7) Elian, M.; Chen, M. M. L.; Mingos, D. M. P.; Hoffmann, R. *Inorg. Chem.* **1976**, *15*, 1148.

(8) Rees, B.; Mitschler, A. *J. Am. Chem. Soc.*, **1976**, *98*, 7918–7924.

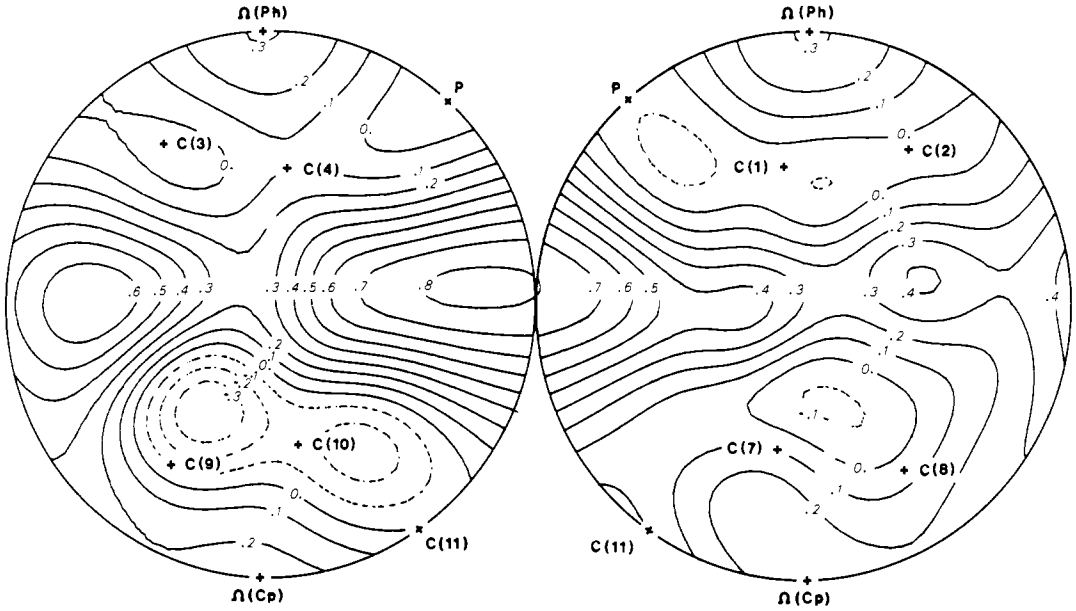

Figure 5. Deformation density on a sphere centered on the iron nucleus (stereographic projection). R = 0.65 Å. The directions from Fe to the other atomic centers of the molecule and to the centers of the two rings are indicated. Contours are as in Figure 2.

phosphaferrocene is quite analogous to ferrocene, where a Mulliken analysis performed at the end of an ab initio calculation[9] had given the following 3d occupancies: z^2 = 1.93; xy and $x^2 - y^2$ = 1.86; xz and yz = 0.43 electrons.

Figure 3 shows the deformation density in the plane defined by the C atoms of the Ph ring. The most interesting feature is the strong accumulation of residual density in the phosphorus region, outside the ring. This peak, which lies essentially in the plane of the ring, is definitely outside the experimental error (peak height 0.82 e Å^{-3}; esd[10] 0.17 e Å^{-3}) and can only be attributed to a localized lone pair on the phosphorus atom.

The fact that the lone pair is near the plane of the five-membered ring seems to indicate that phosphorus behaves as a two-coordinated center and does not take into account the bond with iron. This observation correlates well with the chemical behavior of phosphorus and with the photoelectronic data on similar compounds, which were found analogous to those obtained with genuine two-coordinated phosphorus species.[11]

On the other hand, this is the first time, as far as we know, that a X–X study is carried out on a tervalent organophosphorus derivative. Since, in our case, the lone pair appears to be well localized on phosphorus and nevertheless has lost the greatest part of its nucleophilicity, this suggests a more general comment on the reactivity of tervalent phosphorus compounds. Clearly neither steric hindrance nor global electronic density are sufficient to explain the level of reactivity of a phosphorus lone pair. More sophisticated explanations such as control of the reactivity by frontier orbitals or correlation of the reactivity with the hybridization of phosphorus are needed. Such explanations have been already suggested in many cases (see, for example, ref 11–14), but this is the first time that their need is fully experimentally proven.

Registry No. $(\eta^5\text{-}C_5H_5)[\eta^5\text{-}PC_4H_2(CH_3)_2]Fe$, 63287-56-9.

Supplementary Material Available: A listing of structure factor amplitudes (20 pages). Ordering information is given on any current masthead page.

(9) Coutiere, M.; Demuynck, J.; Veillard, A. *Theor. Chim. Acta* **1972**, *27*, 281. Bagus, P. S.; Wahlgren, U. I.; Almlof, J. *J. Chem. Phys.* **1976**, *64*, 2324–2334.
(10) Rees, B. *Acta Crystallogr., Sect. A* **1978**, *A34*, 254–256.
(11) Guimon, C.; Pfister-Guillouzo, G.; Mathey, F. *Nouv. J. Chim.* **1979**, *3*, 725–729.
(12) Hodges, R. V.; Houle, F. A.; Beauchamp, J. L.; Montag, R. A.; Verkade, J. G. *J. Am. Chem. Soc.* **1980**, *102*, 932–935.
(13) Goetz, H.; Frenking, G.; Marschner, F. *Phosphorus Sulfur* **1978**, *4*, 309–316.
(14) Aue, D. H.; Webb, H. M.; Davidson, W. R.; Vidal, M.; Bowers, M. T.; Goldwhite, H.; Vertal, L. E.; Douglas, J. E.; Kollmann, P. A.; Kenyon, G. L. *J. Am. Chem. Soc.* **1980**, *102*, 5151–5157.